Unified model for formation kinetics of oxygen thermal donors in silicon

Kazumi Wada
Atsugi Electrical Communication Laboratory, Nippon Telegraph and Telephone Public Corporation, Atsugi, Kanagawa 243-01, Japan
(Received 26 August 1983; revised manuscript received 16 April 1984)

A new model is proposed for the formation and decay kinetics of the thermal donors in silicon. This model is an extension of the Kaiser-Frisch-Reiss (KFR) model [Phys. Rev. **112**, 1546 (1958)] and includes the effect of the electronic environment hitherto neglected. The concentration of the thermal donors $n_{TD}(t)$ is expressed by $n_{TD}(t)=(a/b)[O_i]^3 n^{-2}\{1-\exp(-bD_i[O_i]t)\}$, where $[O_i]$ denotes the initial oxygen-interstitial concentration; n, the electron concentration; D_i, the diffusion coefficient of oxygen interstitials; and a and b, constants. Based on this equation, the maximum concentration $[n_{TD}(t=\infty)]_{eq}$ and initial formation rate $[dn_{TD}(t)/dt]_{t=0}$ are expressed, respectively, by $[n_{TD}(t=\infty)]_{eq}=(a/b)[O_i]^3 n^{-2}$ and $[dn_{TD}(t)/dt]_{t=0}=aD_i[O_i]^4 n^{-2}$. The equations are used to derive the annealing-temperature and dopant-concentration dependences as well as the oxygen-concentration dependence of thermal-donor formation. Enhancement of the thermal donor formation in heavily doped, p-type materials and its suppression in heavily doped, n-type materials are theoretically deduced and the latter is experimentally confirmed by deep-level transient (capacitance) spectroscopy (DLTS). It is found that the aggregates with four oxygen atoms are doubly charged donors. It is further suggested that the early aggregates with two or three oxygen atoms would be doubly charged donors and would play the role of the predominant thermal donors in the initial formation stage at a temperature lower than 450 °C.

I. INTRODUCTION

Thermal-donor formation in Czochralski (CZ) grown silicon was discovered by Fuller, Ditzenberger, Hanney, and Buehler in 1954.[1] Kaiser reported the oxygen-interstitial-concentration dependence of thermal-donor-formation kinetics.[2] Based on these results, Kaiser, Frisch, and Reiss related the thermal donors to aggregates of oxygen atoms in silicon, and proposed a model (referred as KFR model) in which the thermal donors consisted of two to four oxygen atoms and in which SiO_4 is predominant.[3] The model satisfactorily explained the oxygen-interstitial-concentration dependence in the formation kinetics of the thermal donors. A large number of investigations have been published in the last 25 years, revealing the fundamental aspects of thermal-donor-formation kinetics.[4] Theoretical efforts have also been made and a few models proposed: the Helmreich-Sirtl model,[5] the Goesele-Tan model,[6] and the Oehrlein-Corbett model.[4] However, no real progress has as yet been made for understanding the various aspects of formation kinetics, such as the annealing-temperature dependence,[7] the dopant-impurity-concentration dependence,[8] the carbon-concentration dependence,[9] etc. No one has paid explicit attention to the roles played by electron concentration in the formation kinetics. It is the purpose of the present paper to explain these dependences and to propose a unified picture including effects of the electronic environment for the formation kinetics of the thermal donors.

II. EXPERIMENTAL OBSERVATIONS

The state of the art of the formation kinetics is briefly summarized in this section.

(1) The initial formation rate of the thermal donors (TD's) in 450 °C annealing is proportional to the fourth power of the interstitial-oxygen concentration $[O_i]$.[2]

(2) The TD's are formed at temperatures between 322 °C and 500 °C, the formation rate peaking at about 450 °C.[7] After attaining the maximum concentration, TD's tend to decrease with time.[7]

(3) The maximum concentration at 450 °C, is proportional to the third power of $[O_i]$.[3,10]

(4) $[n_{TD}(t)]_{eq}$ tends to be higher at lower temperature, but requires longer duration.[7] TD's are easily destroyed by a higher-temperature annealing, so-called donor-killer annealing.[7]

(5) The difference between $[n_{TD}(t)]_{eq}$ and $n_{TD}(t)$ at a certain time at a temperature between 409 °C and 472 °C is proportional to $\exp(-kt)$, where k is a constant and t is an annealing time.[3]

(6) The activation energies of the formation and decay reaction are equal and range between 2.5 and 2.8 eV.[3,7,11,12]

(7) The concentration and formation rate of TD's increases in heavily doped p-type silicon, notably by more than 1×10^{17} atoms/cm^3.[8,9,13,14]

(8) The concentration and formation rate in heavily doped n-type silicon are still controversial: According to Ref. 9, they decrease, according to Ref. 14, there is no change. (This contradiction has not been pointed out in the recent review paper.[4])

(9) The formation rate of TD's is reduced in carbon-rich silicon.[9,15–17]

Information on the physical nature of the thermal donors and various models are reviewed by Oehrlein and Corbett.[4]

III. KINETIC MODEL CONSIDERING EFFECTS OF ELECTRONIC ENVIRONMENT

Thermal donors are suggested to be oxygen aggregates in an early stage of the clustering process in the KFR model. The present model is an extension of the KFR model and first considers electrons generated by thermal-donor formation. In other words, the present model follows the assumption in the KFR model that the aggregates with two to four oxygen atoms are the origin of the thermal donors, and starts from the following defect reactions (see Appendix A):

$$O_i + O_i \underset{k_{-1}}{\overset{k_1}{\rightleftarrows}} A_2^{g+} + ge^- , \tag{1}$$

$$A_2^{g+} + ge^- + O_i \underset{k_{-2}}{\overset{k_2}{\rightleftarrows}} A_3^{h+} + he^- , \tag{2}$$

$$A_3^{h+} + he^- + O_i \underset{k_{-3}}{\overset{k_3}{\rightleftarrows}} A_4^{m+} + me^- , \tag{3}$$

$$A_4^{m+} + me^- + O_i \underset{k_{-4}}{\overset{k_4}{\rightleftarrows}} P_5 , \tag{4}$$

where O_i denotes oxygen interstitials; A_i^{j+}, electronically active oxygen aggregates with i oxygen atoms and j valence electrons (referred simply as A_i); e^-, electron; P_5, electronically inactive oxygen aggregate of five oxygen atoms; k_i and k_{-i}, rate constants from A_i to A_{i+1} and A_{i+1} to A_i, respectively. Note that the term e^- is not involved in the KFR model. The rate equation of thermal-donor formation is generally expressed as

$$dn_{TD}(t)/dt = d[2]/dt + d[3]/dt + d[4]/dt , \tag{5}$$

where $[i]$ denotes concentration of the aggregates with i oxygen atoms. In order to obtain $d[2]/dt$, $d[3]/dt$, and $d[4]/dt$, the mass-action law is applied for reactions (1) and (2), (2) and (3), and (3) and (4), respectively (see Appendix B), assuming that smaller aggregates than the aggregates of interest are in dynamical equilibrium. Then we obtain

$$d[2]/dt = k_1[1]^2 n^{-g} - (k_{-1} + k_2[1])[2] , \tag{6a}$$

$$d[3]/dt = k_2 K_1 [1]^3 n^{-h} - (k_{-2} + k_3[1])[3] , \tag{6b}$$

$$d[4]/dt = k_3 K_1 K_2 [1]^4 n^{-m} - (k_{-3} + k_4[1])[4] , \tag{6c}$$

where [1] denotes the concentration of oxygen interstitials, $[O_i]$; n, electron concentration; and $K_1 = k_1/k_{-1}$ and $K_2 = k_2/k_{-2}$. Thus thermal-donor formation is clearly shown to be affected by the electron concentration n in the present model, in clear contrast to the KFR model.

Under electrical-neutrality conditions, n is expressed as, in n-type specimens,[18]

$$n = 0.5([N_d + n_{TD}(t) - N_a] + \{[N_d + n_{TD}(t) - N_a]^2 + 4n_i^2\}^{0.5}) , \tag{7a}$$

and, in p-type specimens, as

$$n = n_i^2/[0.5([N_a - N_d - n_{TD}(t)] + \{[N_a - N_d - n_{TD}(t)]^2 + 4n_i^2\}^{0.5})] , \tag{7b}$$

where n_i is the intrinsic electron concentration at donor-formation temperature; N_d and N_a, the ionized shallow-donor and -acceptor concentrations, respectively; and $n_{TD}(t) = [2] + [3] + [4]$, the ionized thermal-donor concentration. Furthermore, n_i is expressed as

$$n_i = 4.9 \times 10^{15} (m_{de} m_{dh}/m_0^2)^{3/4} T^{3/2} \exp(-E_g/2k_B T) \tag{8}$$

$$\propto T^{3/2} \exp(-E_g/2k_B T) , \tag{8'}$$

where m_{de} and m_{dh} are the density-of-states effective masses for electrons and holes, respectively; m_0, the free-electron mass; T, the annealing temperature; E_g the energy gap; and k_B, the Boltzmann constant. E_g (in eV) is given by[19]

$$E_g = 1.17 - 4.73 \times 10^{-4} T^2/(T + 636\ \text{K}) , \tag{9}$$

with T given in degrees Kelvin. For simplification, $n_{TD}(t)$ is ignored in Eqs. (7a) and (7b). This simplification is valid when $n_{TD}(t) < n_i$ (e.g., 2×10^{16} cm^{-3} at 450 °C). The condition where $n_{TD}(t) > n_i$ occurs only in very limited cases; for example, at maximum concentration in lightly doped materials annealed at temperatures lower than 450 °C (as will be shown in Fig. 5) or with the oxygen concentration much higher than 1×10^{18} cm^{-3} [from the result (3) in Sec. II]. In the present paper the case of $n_{TD}(t) < n_i$ will be considered. Thus, the time-dependent parameter is the concentration of oxygen aggregates, [2], [3], and [4] in Eqs. (6a), (6b), and (6c), respectively. Therefore, integration of these equations becomes simple, and the concentrations of these aggregates are analytically expressed as

$$[2] = k_1/(k_{-1} + k_2[1])[1]^2 n^{-g}\{1 - \exp[-(k_{-1} + k_2[1])t]\} , \tag{10a}$$

$$[3] = k_2 K_1/(k_{-2} + k_3[1])[1]^3 n^{-h}\{1 - \exp[-(k_{-2} + k_3[1])t]\} , \tag{10b}$$

$$[4] = k_3 K_1 K_2/(k_{-3} + k_4[1])[1]^4 n^{-m}\{1 - \exp[-(k_{-3} + k_4[1])t]\} . \tag{10c}$$

Thus, in the present model, the formation kinetics of aggregates with two to four oxygen atoms are derived.

IV. THEORETICAL DERIVATION OF FORMATION KINETICS

Based on Eqs. (10a)–(10c), the formation kinetics of the thermal donors are theoretically derived in this section.

First, the oxygen-concentration dependences are derived. The formation rate of the thermal donors is given by derivatives of Eqs. (10a), (10b), and (10c), respectively, as follows:

$$d[2]/dt = k_1[1]^2 n^{-g} \exp[-(k_{-1} + k_2[1])t] , \tag{11a}$$

$$d[3]/dt = k_2 K_1 [1]^3 n^{-h} \exp[-(k_{-2} + k_3[1])t] , \tag{11b}$$

$$d[4]/dt = k_3 K_1 K_2 [1]^4 n^{-m} \exp[-(k_{-3} + k_4[1])t] . \tag{11c}$$

The initial formation rate, which is obtained by the sum of Eqs. (11a)—(11c), with $t=0$, is known to be proportional to the fourth power of the oxygen concentration at 450 °C [result (1) in Sec. II]. This indicates that the third term in Eq. (5), i.e., Eq. (11c), is predominant at 450 °C, as already described in the KFR model. We follow the assumption of the KFR model that the aggregates with four oxygen atoms are the thermal donors. Equating t to ∞ in Eq. (10c), the maximum concentration, $[n_{\mathrm{TD}}(t)]_{\mathrm{eq}}$ is given by

$$[n_{\mathrm{TD}}(t)]_{\mathrm{eq}}=[4]^*=[k_3K_1K_2/(k_{-3}+k_4[1])][1]^4n^{-m}\ . \tag{12}$$

Furthermore, since according to the KFR model, $k_{-3}<k_4[1]$, the maximum concentration is given by

$$[4]^*=(k_3K_1K_2/k_4)[1]^3n^{-m}\propto[1]^3\ . \tag{12'}$$

Thus, the result (3) in Sec. II is derived naturally. Therefore it is confirmed that the thermal-donor-formation kinetics on oxygen concentration can be well explained by Eq. (10c) or (11c).

Next, let us derive the annealing-temperature and dopant-concentration dependences of thermal-donor formation. The annealing-temperature dependence results from n (including intrinsic electron concentration), $k_3K_1K_2$, and k_4 in Eq. (11c). The last two factors are assumed to be expressed as follows:

$$k_3K_1K_2=aD_i\ , \tag{13}$$

$$k_4=bD_i\ , \tag{14}$$

where a and b are constants independent of annealing temperature and D_i is the diffusion coefficient of oxygen interstitials. The dopant-concentration dependence results from the electron concentration n in Eq. (11c). Thus the unified equation for the formation kinetics of the thermal donors are finally expressed as

$$n_{\mathrm{TD}}(t)=[4]=a/b[1]^3n^{-m}[1-\exp(-bD_i[1]t)]\ , \tag{15a}$$

or

$$dn_{\mathrm{TD}}(t)/dt=d[4]/dt=aD_i[1]^4n^{-m}\exp(-bD_i[1]t)\ . \tag{15b}$$

The following derivation will be utilized in the next section. According to Eq. (15a), the difference between maximum concentration and concentration at a certain time are derived as

$$[4]^*-[4]=[4]^*\exp(-kt)\ , \tag{16a}$$

$$k=bD_i[1]\ . \tag{16b}$$

Equation (16a) is identical to the equation derived in the KFR model [the result (5) in Sec. II]. When $kt=3$ in Eq. (16a), [4] is nearly equal to $[4]^*$, since $\exp(-3)$ is 0.05. Therefore, the saturation time t_s, which is defined as the time required for attaining the dynamical equilibrium of A_4, is approximately given by

$$t_s=3/k=3/(bD_i[1])\ . \tag{17}$$

TABLE I. Analytical results of the formation kinetics. The following terminology is used in the present paper. $|N_d-N_a|<n_i$, lightly doped materials; $N_d-N_a=N_d\gg n_i$, heavily doped, n-type materials; $N_a-N_d=N_a\gg n_i$, heavily doped, p-type materials. n_i is about 10^{16} cm^{-3} at the donor-formation temperature.

Quantities	Approximated expression	Electronic environment
$[4]^*([n_{\mathrm{TD}}(t)]_{\mathrm{eq}})$	$a/b[1]^3n_i^{-m}$	$\lvert N_d-N_a\rvert<n_i$
	$a/b[1]^3N_d^{-m}$	$N_d-N_a=N_d\gg n_i$
	$a/b[1]^3(n_i^2/N_a)^{-m}$	$N_a-N_d=N_a\gg n_i$
$[d[4]/dt]_{(t=0)}$	$aD_i[1]^4n_i^{-m}$	$\lvert N_d-N_a\rvert<n_i$
	$aD_i[1]^4N_d^{-m}$	$N_d-N_a=N_d\gg n_i$
	$aD_i[1]^4(n_i^2/N_a)^{-m}$	$N_a-N_d=N_a\gg n_i$
t_s	$3(bD_i[1])^{-1}$	Entire range

The analytical results derived from the above considerations are summarized in Table I.

V. COMPARISON WITH EXPERIMENTAL OBSERVATIONS

In this section the theoretical derivations in Sec. IV have been compared to the observed results, (2) and (4)—(8), in Sec. II. The comparisons have been made by multiplying the theoretically obtained thermal-donor concentration by the valence-electron number, except for deep-level transient (capacitance) spectroscopy (DLTS) results, since the previously reported experimental results were mostly shown in electron concentration added by the thermal donors.

A. Annealing-temperature dependence in lightly doped materials

In this subsection we will describe the annealing-temperature dependence of the maximum concentration $[4]^*$ and the formation rate of the thermal donors $d[4]/dt$ in the initial stage.

Figure 1 shows the theoretically calculated [by substituting $t=\infty$ in Eq. (15a)] and experimentally obtained maximum concentration dependences of the thermal donors in lightly doped materials ($|N_d-N_a|<n_i$) on annealing temperature. The experimentally obtained maximum (minimum) concentration of the thermal donors of formation (decay) curve can be regarded as the equilibrium concentration of the thermal donors at a given temperature. Therefore, Fig. 1 includes the minimum-concentration data at 590 °C and after the donor-killer annealing at 650 °C. Hereafter, the maximum (minimum) concentration is referred as the equilibrium concentration. In other words, Fig. 1 shows the solubility of the thermal donors in silicon. It is clearly shown that the equilibrium concentration versus the inverse of temperature gives a linear relationship. The solid and dotted lines are the theoretical calculation results in which m, the number of valence electrons of A_4, is equal to 2 and 1, respectively. The best fit is obtained in the case in which *the thermal*

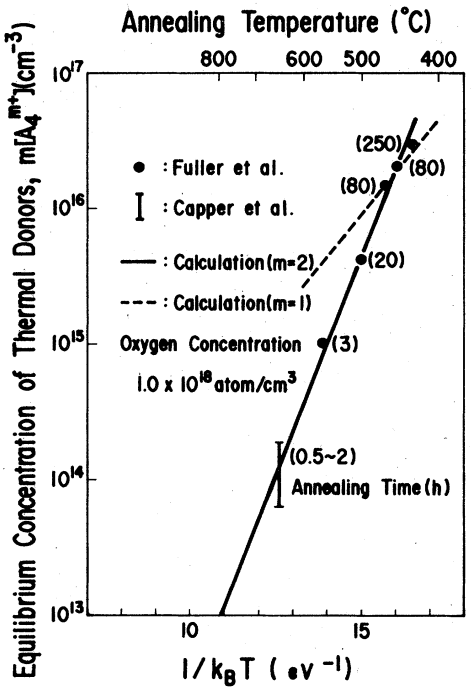

FIG. 1. Equilibrium concentration of the thermal donors versus the inverse of annealing temperature in lightly doped silicon with an oxygen concentration of 1.0×10^{18} cm^{-3}. These data are replotted from the following papers: circles, Ref. 7; bar, Ref. 15. Best fit is obtained when the thermal donors are doubly charged ($m=2$) and $a/b=5.5\times10^{-6}$ in Eq. (15a).

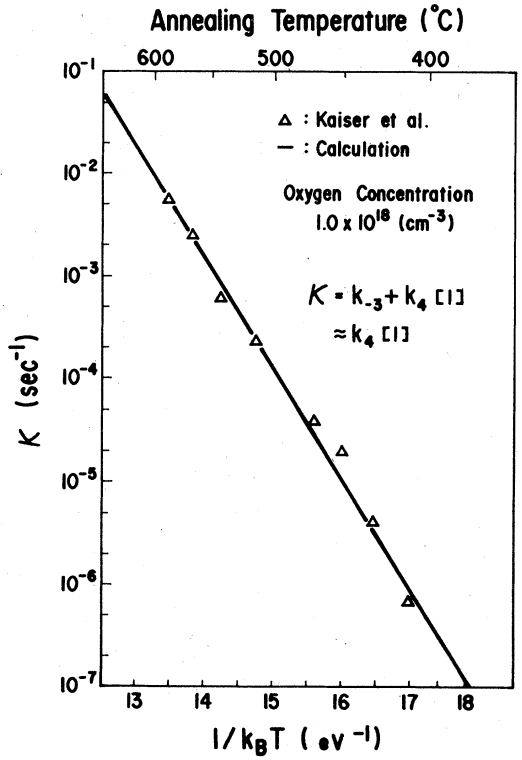

FIG. 2. Experimentally and theoretically determined rate constant k in lightly doped materials. These data are replotted from Ref. 3. Based on Eqs. (16a) and (16b), k is calculated by substituting $D_i=0.17\exp[(-2.54\text{ eV})/k_BT]$ (Ref. 20). The activation energy is 2.54 eV for the data denoted by the solid line, which is consistent with the reported values of 2.5—2.8 eV.

donors are doubly charged ($m=2$), and in which the value 5.5×10^{-6} is assigned to a/b. This result confirms that the annealing-temperature dependence of the equilibrium concentration of the thermal donors results only from the temperature dependence of the intrinsic concentration of electrons, as predicted from Table I. The activation energy is about 1.45 eV in this temperature range, which corresponds to E_g and the term $T^{3/2}$ in Eq. (8′).

Figure 2 shows the theoretically calculated [by using Eq. (16b)] and experimentally determined constant k [the result (5) in Sec. II], versus the inverse of the annealing temperature. The data in Fig. 2 were replotted from Fig. 5 of Ref. 3. In order to fit Eq. (16b), we must first substitute the diffusion coefficient of oxygen interstitials at the given donor-formation temperatures of 400—600 °C into Eq. (16b). Fortunately, Stavola, Patel, Kimerling, and Freeland have recently reported the diffusion coefficient of oxygen interstitials in their dichroism experiment at donor-formation temperatures.[20] They measured reorientation lifetimes in dispersed specimens at 1350 °C, corresponding to the following diffusion coefficient in the temperature range 270—400 °C:

$$D_i=0.17\exp[(-2.54\text{ eV})/k_BT]\ , \tag{18a}$$

which is in good agreement with the extrapolated value measured at higher temperature.[20] Shown in Fig. 2 is the calculation in which the diffusion coefficient, Eq. (18a), is substituted into D_i. The theoretical line is calculated with b [in Eq. (16b)] equal to 5.0×10^{-5} cm^4. The theory fits the experimental data very well. The activation energy of k is equal to that of the oxygen diffusion coefficient, 2.54 eV, for the line, which agrees well with the experimentally obtained values of 2.5—2.8 eV shown in the result (6) in Sec. II. This confirms that the diffusion of oxygen interstitials is responsible for thermal-donor formation. However, the value of the oxygen diffusion coefficient obtained from the kinetics must be 2 orders of magnitude larger than Eq. (18a), as pointed out by Kaiser *et al.*[3] Stavola *et al.* have reported fast reorientation observed in as-provided specimens (preannealed at 900 °C for 2 h),[20] which corresponds to the following diffusion coefficient:

$$D_a=3.2\times10^{-4}\exp[(-1.96\text{ eV})/k_BT]\ , \tag{18b}$$

which is about 2 orders of magnitude higher than Eq. (18a) at the donor-formation temperatures. However, it seems unlikely that this fast diffusion can fulfill the value of the diffusion coefficient of oxygen interstitials calculated from the thermal-donor-formation kinetics, since the activation energy is inadequate [the result (6) in Sec. II] and a good fit cannot be obtained in Fig. 2. Furthermore, Fuller *et al.* explained that their specimens were dispersed above 1200 °C before donor-formation annealing.[7] Therefore, their experimental condition is similar to the condition where the oxygen diffusion coefficient, Eq. (18a), was obtained. Hereafter, the diffusion coefficient, Eq. (18a), is therefore employed in the present paper, although the

problem concerning the oxygen diffusion coefficient still remains.

Next, let us examine the initial formation rate. Figure 3 shows the initial formation rate of the thermal donors calculated by substituting $t=0$ into Eq. (15b) with the experimental data. The data are obtained by dividing the measured thermal-donor concentration by the examined shortest annealing time, 5 h, appearing in Fig. 7 of Ref. 7. Here we note that A_4 is assumed to be a unique origin of thermal donors. This assumption should be valid at least at 450°C, according to the oxygen-concentration dependence [result (1) in Sec. II]. Therefore the constant a is calculated by fitting at 450°C. The solid line is the theoretical calculation result, employing $m=2$ and $a=2.8\times10^{-10}$ cm^4. Thus, a/b and b have been independently obtained from the different sources in Figs. 1 and 2. Therefore, a can be obtained by simple calculation to be 2.75×10^{-10} cm^4, which compares favorably to that value obtained above. The internal consistency in the present model is very good. In serious contrast, no internal consistency was obtained in the case in which the thermal donors are singly charged ($m=1$). The experimental results shown in Fig. 3 are smaller in the higher-temperature range and slightly larger in the lower-temperature range than expected from the present model. Let us show that the cause of the discrepancy is explained in terms of the time-dependent formation rate in the higher-temperature region and the contribution of the early aggregates A_2 and/or A_3 in the lower-temperature region in the following. The calculated result for t_s by Eq. (17) is shown in Fig. 4. The experimentally obtained data are plotted from Fig. 7 of Ref. 3. The data are in good agreement with the calculation, which also shows that the present model predicts the formation kinetics very well. It is readily found from Fig. 4 that t_s is shorter than 5 h above 500°C. This indicates that the initial formation rates experimentally determined around 500°C at 5 h have been influenced by saturation of thermal-donor formation and consequently underestimated. In order to obtain a more rigorous formation rate in the initial stage, we have made the following correction (correction A). Based on Eq. (15b), the ratio R, the initial formation rate ($t=0$) divided by the formation rate after annealing for 5 h ($t=5\times3600$ sec), is given by

$$R=\exp(bD_it)\,|_{(t=5\times3600)}\,. \tag{19}$$

Thus the initial formation rate is given by multiplying the data in Fig. 3 by R. The data modified by the "correction A" are shown by open circles. The data at temperatures above 450°C agree well with the calculation shown by the solid line. This indicates that the initial formation rate of A_4 is successfully derived from the present model above 450°C. However, the data at lower temperatures are still higher than the calculated data, since correction A becomes negligible at temperatures lower than 450°C. It is

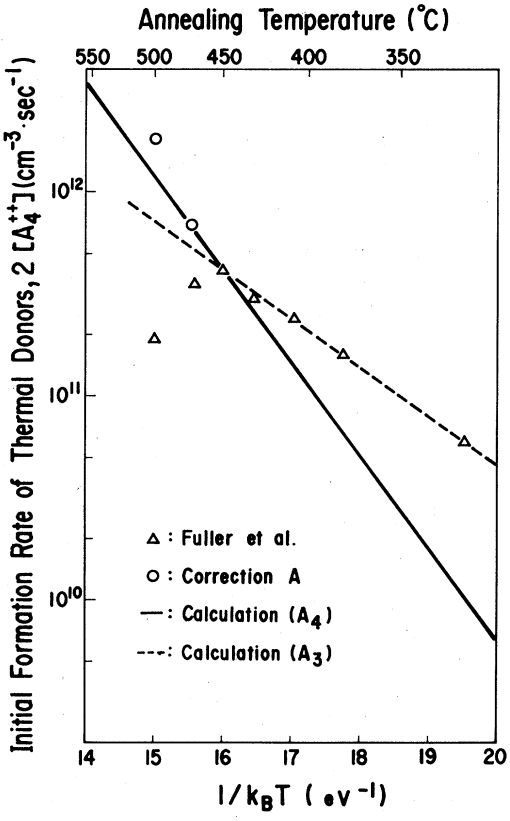

FIG. 3. Initial formation rate of the thermal donors versus the inverse of temperature. Triangles are from Ref. 7. Data are obtained by dividing the measured thermal-donor concentration at 5 h by the 5 h appearing in Fig. 7 of Ref. 7. The solid line is calculated by using Eq. (15b) with $a=2.8\times10^{-10}$ cm^4. Based on Eq. (19), correction A is done for all data and the data changed remarkably are shown as open circles. The dotted line shows the theoretically determined initial formation rate of the early aggregates A_3, assuming that A_3 is doubly charged and the rate-determining diffusion coefficient is Eq. (18b).

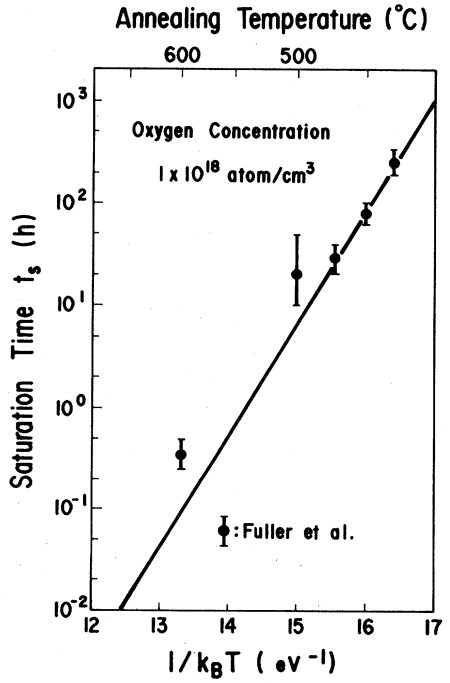

FIG. 4. Saturation time versus the inverse of temperature. The solid line is calculated by using Eq. (17). The experimental data are replotted from Fig. 7 of Ref. 7.

shown below that the enhancement below 433 °C can be derived under the assumption that the early aggregates, A_2 or A_3, are the predominant thermal donors. In the initial stage the early aggregates are not considered to be in dynamical equilibrium, especially at low temperature. Therefore, it is inferred that concentration of A_4 is very small and the early aggregates predominantly play the role of thermal donors at temperatures lower than 433 °C. Assuming that A_2 is in dynamical equilibrium, A_3 plays roles in the low-temperature region. Based on Eq. (11b), the formation rate of A_3 is given by

$$d[3]/dt = cD_i[1]^3 n^{-h} \exp(-dD_i[1]t) , \tag{20}$$

with similar assumptions to those in the case of A_4,

$$k_2 K_1 = cD_i , \tag{21}$$

$$k_3 = dD_i , \tag{22}$$

$$k_3[1] > k_{-2} . \tag{23}$$

For simplification, the formation rate of A_3 in the initial stage is assumed to be equal to that after annealing for 5 h. In other words,

$$d[3]/dt = cD_i[1]^3 n^{-h} . \tag{20'}$$

The dotted line is calculated by substituting 2 into h, and D_a, Eq. (18b), into D_i in Eq. (20'), with $c = 2 \times 10^{-7}$ cm^{-2}, and it agrees well with the data in this temperature region. This suggests that the early aggregates are also doubly charged donors and the reaction is governed by the fast-diffusion coefficient, Eq. (18b). Furthermore, the oxygen-concentration dependence of the initial formation rate at temperatures lower than 433 °C will clarify whether A_2 or A_3 is the predominant thermal donor in this temperature range. Kaiser *et al.* reported the appearance of a nonlinear relationship in $\ln([4]^* - [4])$ versus annealing time observed at 433 °C and 409 °C in the initial formation stage, as shown in Fig. 2 of Ref. 3. The nonlinear relationship corresponds to the enhancement of the initial formation rate observed in Fig. 3. The result of Kaiser *et al.* just indicates the effect of the early-aggregate presence, whereas the present result discusses it on a quantitative basis. However, some reports have suggested that the early aggregates would be acceptors.[21,22] It might be premature to discuss this subject any further without detailed experimental information. Experimental efforts should be focused on the formation kinetics and the electrical activity of the early aggregates.

B. Dopant concentration and annealing-temperature dependence on heavily doped materials

Figures 5–9 show the calculated and experimentally obtained dopant-concentration and annealing-temperature dependences of the equilibrium concentration and the initial formation rate, calculated from Eqs. (15a) and (15b), using the constants a and b determined in the preceding subsection. As far as the thermal-donor concentration in

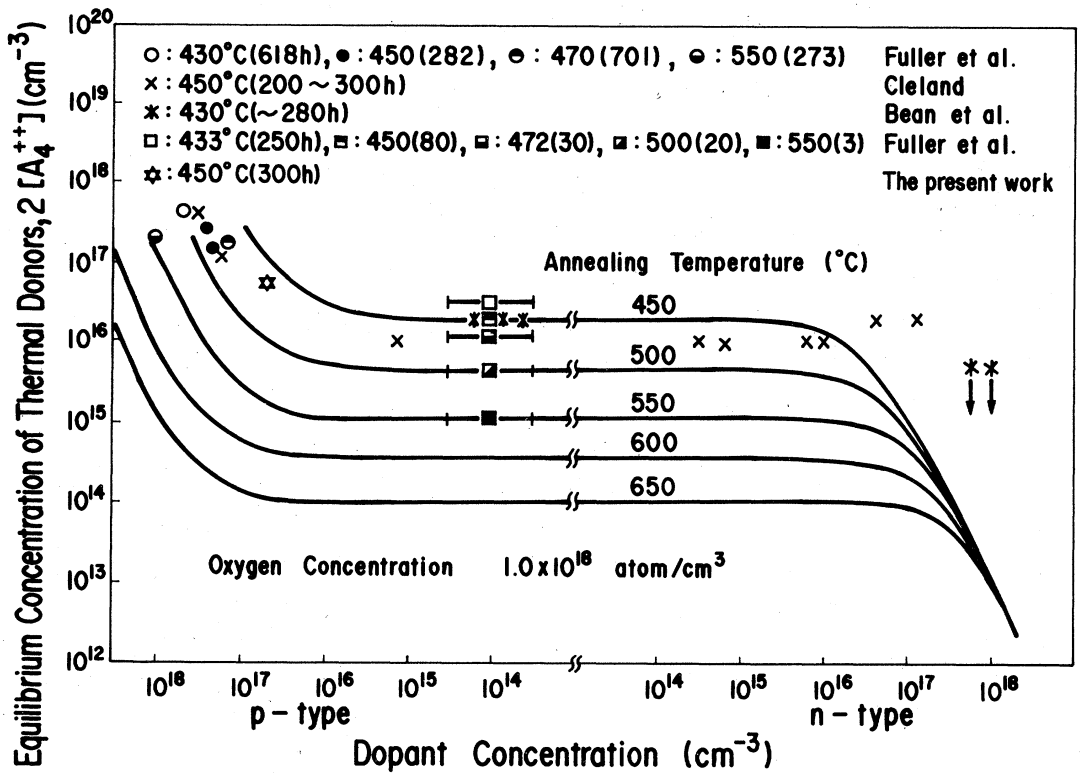

FIG. 5. Equilibrium concentration dependence on dopant concentration. The data are replotted from the following reports: circles, Ref. 8; crosses, Ref. 14; asterisks, Ref. 9; squares, Ref. 7; stars, the present work. The data in heavily doped, p-type materials agree well with the present model. The data are controversial in heavily doped, n-type materials, but the data (asterisks) indicating strong reduction agree with this calculation.

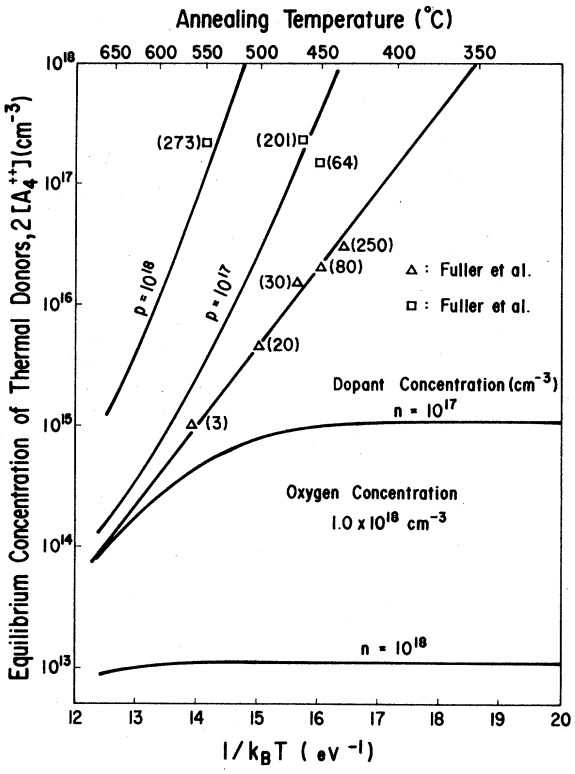

FIG. 6. Equilibrium concentration dependence on the inverse of annealing temperature. The data are replotted from the following reports: triangles, Ref. 7; squares (1.1×10^{18} B atoms cm^{-3} and 1.6×10^{17} Al atoms cm^{-3}), Ref. 8. As for n-type materials, there is no reliable data. The numbers adjacent to these marks indicate the annealing time in hours.

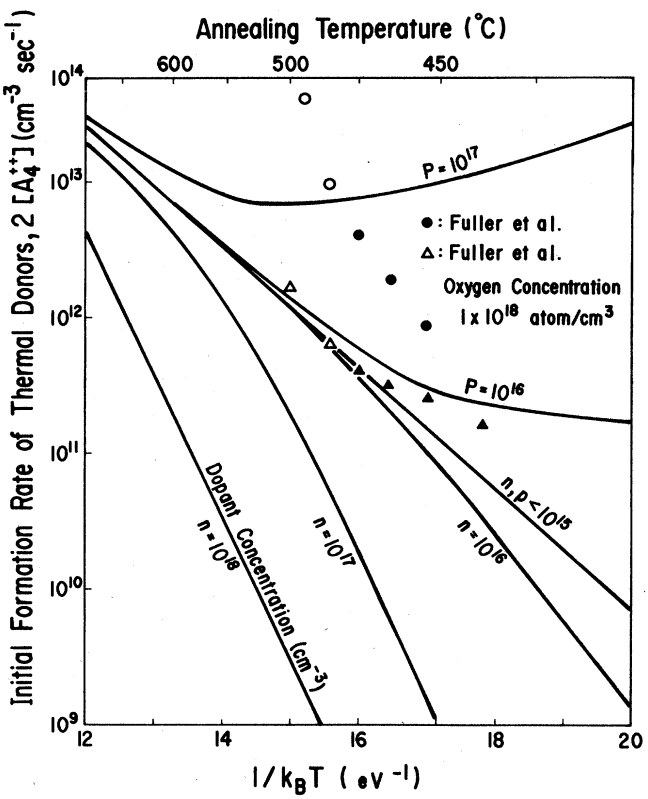

FIG. 8. Initial formation-rate dependence on dopant concentration. The data are from the following reports: triangles, Ref. 7; circles, Ref. 8 (6.3×10^{17} Al atoms cm^{-3}). These data are data corrected by using correction A.

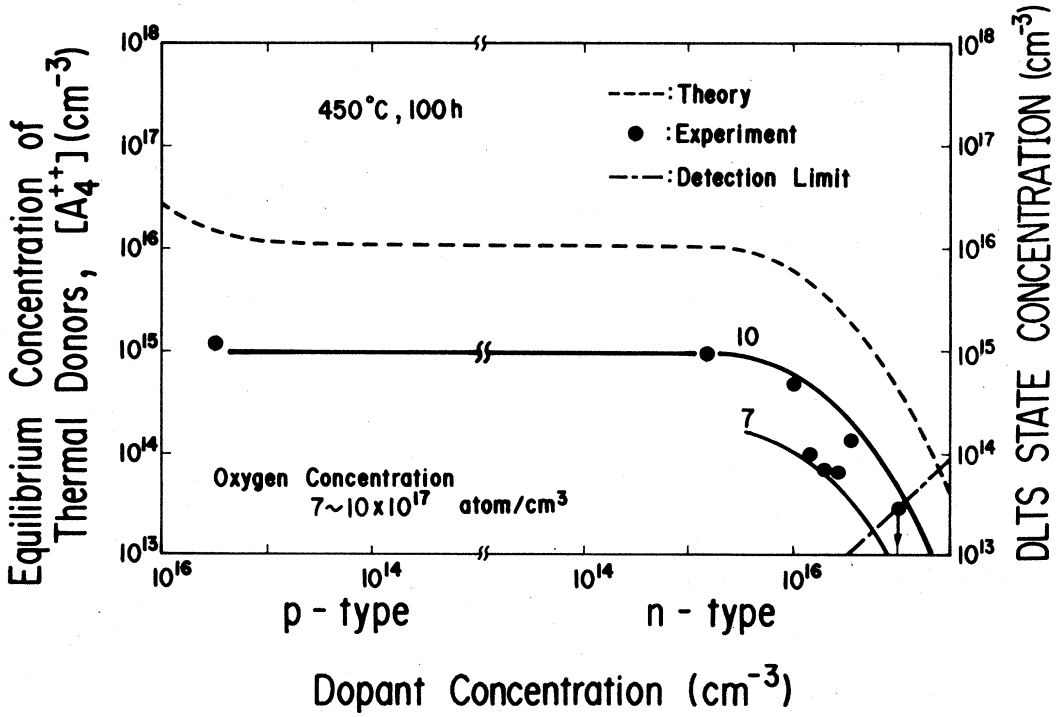

FIG. 7. Experimentally obtained equilibrium concentration dependence on the dopant-concentration dependence. The concentration of $E_c-0.15$ eV states was obtained by DLTS measurements on materials annealed at 450 °C for 100 h.

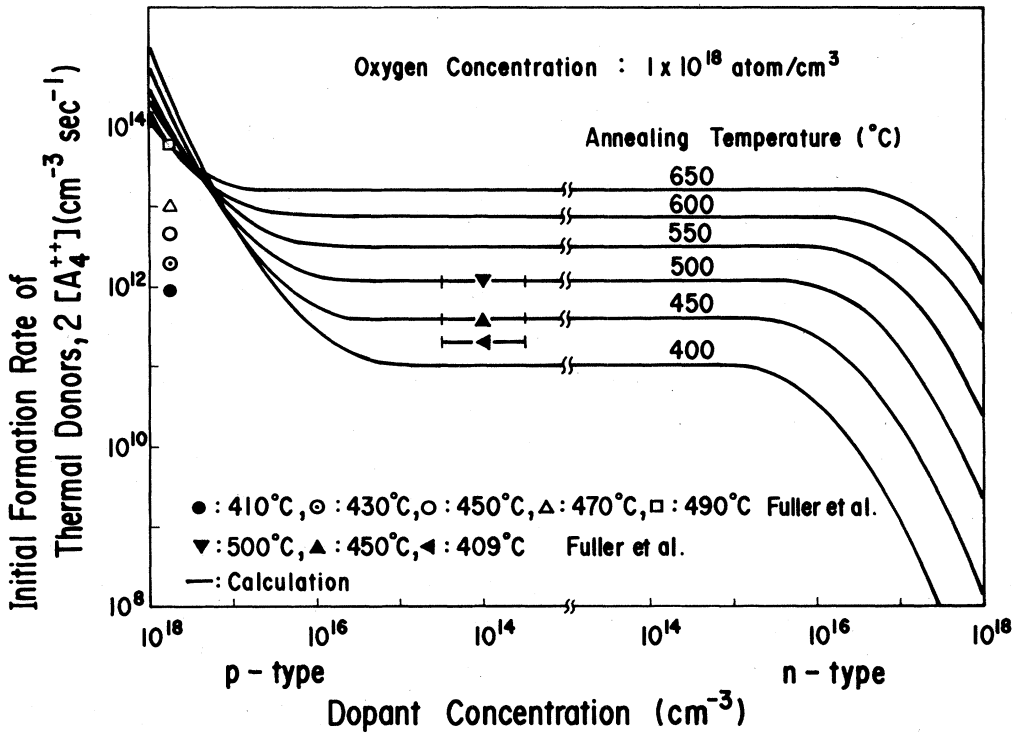

FIG. 9. Initial formation-rate dependence on the inverse of annealing temperature. The data are from the following reports: Ref. 8 for heavily doped, p-type materials and Ref. 7 for lightly doped materials. These data are corrected by correction A.

the heavily doped, p-type materials is concerned, the fitting is quite nice, as shown in Figs. 5 and 6. A saturation in the equilibrium concentration toward 5×10^{17} cm^{-3} in the heavily doped p-type region in Fig. 5 is observed. It is quite natural that no thermal donors are formed with more than one-quarter of the initial oxygen-interstitial concentration, since one thermal donor needs at least four oxygen atoms in the case of A_4. The present model indicates that there should be a strong reduction in the thermal-donor concentration in heavily doped n-type materials. (For example, the thermal-donor formation should be almost entirely suppressed in the materials with n-type dopant and of concentration 10^{18} cm^{-3}.) However, the data in heavily doped n-type materials, as shown in Fig. 5, are controversial. Figure 7 shows the experimentally determined concentration dependence of the thermal donors on dopant concentration.[23] The thermal donors were formed by 450°C annealing for 100 h, and the concentration was measured by DLTS on Au Schottky-barrier diodes.[24] As shown in Fig. 4, the thermal-donor concentration extends to its equilibrium concentration. Oxygen concentrations in these materials were (10—7) $\times10^{17}$ atoms/cm^3 and were 8 and 7×10^{17} atoms/cm^3 in the n-type materials doped with more than 1×10^{16} cm^{-3} of dopant. It is clearly found that thermal-donor formation is suppressed with increasing n-type dopant concentration. It can be said that the predictions by the present model are verified with respect to the equilibrium concentration of the thermal donors.[25]

Figures 8 and 9 show the annealing-temperature and dopant-concentration dependences of the initial formation rate. It must be noted that experimental data of the initial formation rate on heavily doped, p-type materials are quite few and no data are available on heavily doped, n-type materials. The data in these figures are obtained by dividing the thermal-donor concentration in Fig. 5 of Ref. 8 by 5 h. Correction A was performed. It is readily found that the initial formation rates are enhanced in heavily doped, p-type materials, as shown in these figures. However, fitting does not appear to be very good in Figs. 8 and 9, in comparison with that in the previous figures. The calculation is always smaller than the data. This may result from the experimental error as follows. In heavily doped, p-type materials, the concentration of the thermal donors was determined by subtracting hole concentration after annealing from that before annealing. It is easily understood that this procedure would result in a large measurement error, especially in the initial stage because of the small concentration of the thermal donors. As noted above, there is serious experimental difficulty in the measurement of the initial formation rate in heavily doped p-type materials.

In summary, the present model explains results (1)—(8) in Sec. II fairly well as follows.

(1) The equilibrium concentration dependences on annealing temperature and dopant concentration are well explained. The suppression of the thermal donors is predicted and experimentally verified in heavily doped, n-type materials.

(2) The initial-formation-rate dependences on annealing temperature and dopant concentration are well explained

TABLE II. Results obtained by comparison of theory and experiment.

Quantity	Thermal donor	Valency	Temperature range (°C)	Dopant concentration range
Equilibrium concentration	A_4	2	$433 < T < 650$	Entire range
Initial formation rate	A_4	2	$T > 450$	Lightly doped
	A_3 or A_2	2	$T < 433$	No reliable data in heavily doped materials.

in lightly doped materials. The dependences in heavily doped materials are not explained very well, which is presumably due to some experimental problems.

(3) The aggregates A_4 are concluded to be doubly charged donors acting as primary thermal donors. The early aggregates A_2 or A_3 are suggested to be doubly charged donors acting as primary donors in the initial formation stage in low-temperature annealing.

These results are summarized in Table II. Further experimental efforts are expected to be made for making this new model totally convincing, especially in the initial formation rate in heavily doped materials and in the formation kinetics and electrical properties of the early aggregates.

VI. DISCUSSION

A. Nature and formation kinetics of thermal donors

The physical nature of thermal donors is not clarified in the present model. However, the present model strongly supports that idea that the thermal donors are oxygen aggregates, since the formation kinetics of the thermal donors depending on oxygen concentration, annealing temperature, and dopant concentration are satisfactorily explained by the present model extended from the KFR model. However, the largest problem in the models based on oxygen aggregates still remains: The anomalously high oxygen diffusion coefficient determined by the formation and decay kinetics of the thermal donors, as already noted by Kaiser *et al.*[3] We have shown that the formation kinetics of A_4 cannot be explained without about a hundred-times-higher oxygen diffusion coefficient with the same activation energy, 2.54 eV, of "slow" oxygen diffusion. In contrast, the formation kinetics of the early aggregate A_3 (or A_2) can be explained by the fast-diffusion coefficient with the activation energy, 1.96 eV, reported by Stavola *et al.* Based on this result, we would propose that the origin of the thermal donors are oxygen aggregates, but that the diffusion of oxygen interstitials is modified by some mechanism related to the point-defect diffusion. We must conclude this discussion of the problem of diffusion modulation by introducing the fact that both Goesele and Tan[5] and Pajot *et al.*[26] have proposed that oxygen molecules and Si=O molecules are fast-diffusion vehicles for oxygen atoms and the thermal donors, respectively. Further efforts are quite necessary.

The electronic nature of the thermal donors has not been clarified yet. In other words, it was not clearly understood whether two well-known states, $E_c - 0.07$ eV and $E_c - 0.15$ eV,[24] were produced by formation of doubly charged donors or by formation of two independent, singly charged donors. The present model clarifies, from the kinetics information, that the thermal donors are doubly charged donors. Therefore it is indicated that these two states are the ionized states of one thermal donor. Recently, electronic transitions of the thermal donors has been detected by infrared- (IR-) absorption measurements at extremely low temperatures.[10,27,28] The present result is consistent with the interpretation of the IR-absorption results based on the effective-mass theory.[29] Furthermore, at least nine transitions, presumably based on the different donors, have been detected, and their intensity (concentration of each thermal donor) dependence on annealing time has been obtained.[28] One-to-one correspondence between their electronic transitions and oxygen aggregates will illuminate the initial stage of oxygen aggregation and contribute a clue toward solving the mystery of thermal-donor problems.

One cautionary note we wish to point out is that the present model is still valid in the case in which aggregates with more than five oxygen atoms are electrically active, since Eqs. (6a)—(6c) are not changed by this modification. It is assumed that the concentration of these (late) aggregates with more than five oxygen atoms would be smaller than that of A_4.

Finally, we would like to mention the mechanism of donor-killer annealing. Up to now the mechanism has been speculated on, but not understood. However, the present model gives a satisfactory explanation for the mechanism based on the solubility limit of the thermal donors shown in Fig. 1. Further problems to be solved are (1) the anomalous diffusion coefficient of oxygen interstitials calculated from the formation kinetics, (2) the suppression effect by carbon, and (3) the electrical activities and formation kinetics of the early and/or late aggregates.

B. Thermal-donor formation during cooling of crystal growth

The thermal-donor concentration in as-grown crystals, i.e., the formation process during cooling of crystal growth, will be predicted from the present model. In lightly doped crystals the equilibrium concentration of the

thermal donors is low since the annealing temperature is high, as shown in Fig. 1. Therefore, the thermal donors will begin to become visible at temperatures lower than 800 °C, where the equilibrium concentration is about 10^{13} cm^{-3}. The initial formation rate at this temperature is extremely high (the saturation time is very short, as shown in Fig. 4) and sufficient to attain the equilibrium concentration in a short time. However, as the crystal is cooled, the equilibrium concentration becomes higher, but the formation rate lower. As a result, thermal-donor formation ceases at a certain temperature. Thermal donors, with a concentration of 10^{15} cm^{-3}, are often involved in as-grown crystals with an oxygen concentration of 10^{18} cm^{-3}. Their concentration is equal to the equilibrium concentration at 550 °C, where the saturation time is clearly shorter than 1 h, as shown in Fig. 4. Therefore, thermal-donor formation ceases at about 550 °C in the zeroth-order approximation. In contrast, the situation is considerably different in heavily doped crystals. In heavily doped, p-type crystals, the equilibrium concentration and the initial formation rate are strongly enhanced, as shown in Figs. 5–9. Therefore, the onset temperature of thermal-donor formation should be higher than 800 °C and the cessation temperature lower than 550 °C, resulting in the presence of a high concentration of thermal donors in as-grown crystals. In heavily doped, n-type crystals, the situation is totally opposite, and therefore the thermal-donor concentration is lower in as-grown crystals than in lightly doped crystals. For example, the equilibrium concentration of the thermal donors is calculated to be only 1×10^{13} cm^{-3} in crystals with n-type dopant of concentration 10^{18} cm^{-3}. Therefore, no thermal donors should be actually observed in as-grown, heavily doped, n-type crystals because of the detection limit.

C. Electronically enhanced defect reaction

Research on defects in semiconductors is now in a period of heightened activity throughout the world. Electronically enhanced defect reactions are now the most active area in this research field. The electronic enhancement effects are classified into three categories: Electric field effect, charge-state effect, and recombination-enhancement effect. As for the thermal-donor formation, the first effect found to be manifested as the Poole-Frenkel effect on the level of the thermal-donor state.[24] The charge-state effect has been quantitatively understood by the present model, but the recombination-enhancement effect is not reported since silicon devices do not utilize recombination phenomena. In addition to thermal-donor formation, dislocation-velocity enhancements reported by Erofeev *et al.*[30] and Patel *et al.*,[31] and enhancement and depletion of swirl defects and oxide precipitates reported by deKock *et al.*,[32,33] have been reported. However, mechanisms for these phenomena are still known.

Now let us consider the origin of the enhancement and depletion of swirl defects and oxide precipitates. deKock *et al.* have experimentally studied doping effects on swirl-defect formation during crystal growth and found that microdefect formation is suppressed by n-type doping and enhanced by p-type doping.[32] They also have recently reported that after 1000 °C annealing the precipitate density is lower in heavily doped, n-type crystals and higher in heavily doped, p-type crystals.[33] Pearce *et al.*[34] and Tsuya *et al.*[35] have confirmed these results. Based on the present model, an interrelationship between thermal-donor formation and precipitation in silicon can explain the enhancement and depletion phenomena as follows. I consider it likely that the thermal donors, i.e., the aggregates with two to four oxygen atoms, are "embryos" or stable precipitates in oxide precipitate nucleation. Furthermore, it must be emphasized that oxide precipitates cannot be nucleated without passing through the thermal donors in homogeneous nucleation. In addition, it is well accepted that the oxide precipitates are primary defects and the other microdefects, such as stacking faults and dislocation loops (including swirl defects), are secondary defects nucleated at the precipitates.[36] Therefore, it seems likely that the densities of the oxide precipitates and the secondary defects in as-grown crystals and annealed materials are eventually determined by the thermal-donor-concentration in as-grown crystals and the concentration before annealing, respectively, provided the homogeneous nucleation is the predominant process in oxygen precipitation in CZ silicon. As has been clarified in the present paper, the thermal-donor concentration is strongly affected by dopant type and concentration in heavily doped crystals. Therefore it is predicted that these microdefect densities in as-grown crystals or after annealing would be considerably higher in heavily doped, p-type crystals ($N_a-N_d\gg10^{16}$ cm^{-3}) and lower in heavily doped, n-type crystals ($N_d-N_a\gg10^{16}$ cm^{-3}), in comparison with lightly doped crystals. This prediction is consistent with the experimental observations noted above. In contrast, deKock *et al.* and the other workers have often tried to argue that these microdefect formations are related to intrinsic point defects, vacancies, and self-interstitials whose concentration is assumed to change with dopant type and concentration. They have inferred that the equilibrium concentration of negatively charged self-interstitials would be higher in heavily doped, p-type materials and lower in heavily doped, n-type materials, which is the same tendency of the enhancement and depletion of A swirls (suggested to be interstitial-type dislocation loops) as well as oxygen precipitation in heavily doped materials, respectively. However, no direct evidence has been reported to show that the concentration of these intrinsic point defects is altered by doping level, nor that self-interstitials favor a negatively charged state. It seems fair to say that both possibilities should be carefully examined before the anomalous precipitation phenomenon in heavily doped crystals is quantitatively understood.

VII. CONCLUSION

The present model extended from the Kaiser, Frisch, and Reiss model succeeds at giving a unified explanation for the formation kinetics of thermal donors: oxygen-concentration dependence, annealing-temperature dependence, and dopant-concentration dependence. Most of the formation kinetics are explained by assuming that the aggregates with four oxygen atoms act as the thermal

donors. The unified expression for the formation kinetics is

$$n_{TD}(t)=[4]=(a/b)[O_i]^3 n^{-2}[1-\exp(-bD_i[O_i]t)] ,$$

where $n_{TD}(t)$ denotes the concentration of the thermal donors; [4], the concentration of aggregates with four oxygen atoms; O_i, the oxygen concentration; n, the electron concentration; D_i, the oxygen diffusion coefficient; t, the annealing time; and a and b, constants. It is found, from fitting the model with the experimental observations reported previously, that

$$[n_{TD}(t)]_{eq}=[4]^* \propto [O_i]^3 n^{-2} ,$$

$$[n_{TD}(t)/dt]_{(t=0)}=[d[4]/dt]_{(t=0)} \propto D_i[O_i]^4 n^{-2} ,$$

where the subscript eq denotes equilibrium. The annealing-temperature dependence reflects that of the diffusion coefficient of oxygen interstitials and the intrinsic electron concentration. The dopant-concentration dependence results from the electron concentration determined by the electrical-neutrality condition. The analysis indicates that the aggregates with four oxygen atoms are doubly charged donors, and suggests that the early aggregates with two or three oxygen atoms are doubly charged as well. It is confirmed that the early aggregates play an important role in the initial formation stage at temperatures lower than 450 °C in lightly doped materials. A new interpretation is proposed for the anomalous phenomena of defect formation in heavily doped crystals during cooling of crystal growth and/or annealing, related to the enhancement and depletion phenomena of the thermal donors in as-grown crystals.

ACKNOWLEDGMENTS

The author is grateful to K. Murai of Japan Silicon Co. Ltd. for supplying partly used wafers, and is very much indebted to N. Inoue for his suggestion on anomalous precipitation phenomena in heavily doped materials. He also thanks T. Izawa for his encouragement throughout this work.

APPENDIX A

The basic reactions for the formation of A_2^{2+}, Eq. (1), are expressed as

$$O_i+O_i \rightleftarrows A_2 , \quad \text{(A1)}$$

$$A_2 \rightleftarrows A_2^+ + e^- , \quad \text{(A2)}$$

$$A_2^+ \rightleftarrows A_2^{2+} + e^- . \quad \text{(A3)}$$

To simplify matters, assume that the valency of A_2 is 2. Similarly, Eqs. (2)—(4) can be expressed. The equilibrium constants K, K^+, and K^{2+} for Eqs. (A1)—(A3) is expressed by

$$K=[A_2]/[O_i]^2 . \quad \text{(A4)}$$

$$K^+=[A_2^+]n/[A_2] , \quad \text{(A5)}$$

$$K^{2+}=[A_2^{2+}]n/[A_2^+] . \quad \text{(A6)}$$

It can be seen from Table III in Appendix B that Fermi level is always a few k_BT lower lying below the energy level of the thermal donors, $E_c-0.07$ eV and $E_c-0.15$ eV, except for the case of an electron concentration of 10^{18} cm^{-3} at 300 °C annealing. In other words, the specimens with an electron concentration lower than 10^{18} cm^{-3} are saturated or in an intrinsic range during annealing at temperatures higher than 300 °C. Typical examples have been shown using Hall-effect measurement.[10,11] This means that K^+ and K^{2+} are temperature-independent constants, and A_2 is completely ionized at the donor-formation temperature,

$$O_i+O_i \rightleftarrows A_2^{2+}+2e^- . \quad \text{(A7)}$$

Thus, basic reactions for the formation of A_2^{g+}, A_3^{h+}, and A_4^{m+} can be written as Eqs. (1)—(4).

APPENDIX B

Classical statistics, not Fermi-Dirac statistics, should be used in the derivation of the temperature dependence of the defect reaction we are concerned with.[37] In other words, the equilibrium constants in Eqs. (6a)—(6c) should be constant at a given temperature and independent of solute concentration. Now let us examine whether or not Fermi-Dirac statistics may be approximated to classical statistics in the present case. The criteria are $E_d-E_f > k_BT$ and $E_c-E_F > k_BT$, where E_d, E_F, and E_c denotes the donor level, Fermi level, and the bottom of the conduction band, respectively, and k_B is the Boltzmann constant and T is the annealing temperature. These criteria will be fulfilled when the annealing temperature is reasonably high, the donor level is not too deep, and the

TABLE III. E_d-E_F dependence on the annealing temperature and carrier concentration in n-type materials. E_d-E_F is always larger than k_BT at the donor-formation temperature, except at 300 °C and at a concentration of 10^{18} cm^{-3} of n-type dopants. The values E_c-E_F used are 0.07 and 0.15 eV, as reported by Kimerling and Benton (Ref. 24).

Temperature (°C)	k_BT (eV)	E_d-E_F (eV) Electron concentration (cm^{-3}) 10^{18}	10^{17}	10^{16}	10^{15}	10^{14}
300	0.049	0.04	0.15	0.27	0.35	0.37
400	0.058	0.09	0.22	0.32	0.35	0.35
500	0.067	0.13	0.28	0.33	0.33	0.33
600	0.075	0.18	0.29	0.31	0.32	0.32
700	0.084	0.22	0.29	0.29	0.30	0.30

equilibrium concentration is not too large. The last two factors are satisfied in the present case. However, the first factor is not explicitly valid. Therefore, it might be necessary to check it. As shown by DLTS measurements,[24] there are two states, $E_c-0.07$ eV and $E_c-0.15$ eV, for the thermal donors. Although these states become shallower as the annealing time becomes longer,[12] these states are referred to as $E_c-0.07$ eV and $E_c-0.15$ eV in this work. It is sufficient to check that the deeper states are located sufficiently higher than the Fermi level. Therefore, E_d can be considered to be $E_c-0.15$ eV. It is readily understood that since E_c-E_F in p-type materials is larger than half of the energy gap, the criteria are fulfilled quite naturally. Table III summarizes the temperature dependence of E_d-E_F with carrier concentration in n-type materials. The calculated E_d-E_F value is always larger than k_BT, except for the cases of an electron concentration higher than 1×10^{18} cm^{-3} at temperatures lower than 300 °C. It is therefore concluded that classical statistics are applicable in the present case instead of Fermi-Dirac statistics, and that the analysis of the defect chemistry with the law of mass action is valid.

[1]C. S. Fuller, J. A. Ditzenberger, N. B. Hanney, and E. Buehler, Phys. Rev. **96** 833 (1954); and Acta Metall. **3**, 97 (1955).

[2]W. Kaiser, Phys. Rev. **105**, 1751 (1957).

[3]W. Kaiser, H. L. Frisch, and H. Reiss, Phys. Rev. **112**, 1546 (1958).

[4]See, for example, as a review, G. S. Oehrlein and J. W. Corbett, in *Defects in Semiconductors II,* edited by S. Mahajan and J. W. Corbett, (Elsevier, New York, 1983), p. 107.

[5]D. Helmreich and E. Sirtl, in *Semiconductor Silicon 1977,* edited by H. R. Huff and E. Sirtl (The Electrochemical Society, Princeton, New Jersey, 1977), p. 626.

[6]U Goesele and T. Y. Tan, Appl. Phys. A **28**, 564 (1982).

[7]C. S. Fuller and R. A. Logan, J. Appl. Phys. **28**, 1427 (1957).

[8]C. S. Fuller, F. H. Doleiden, and K. Wolfstirn, J. Phys. Chem. Solids **13**, 187 (1960).

[9]A.R. Bean and R. C. Newman, J. Phys. Chem. Solids **33**, 255 (1972).

[10]D. Wruck and P. Gaworzewski, Phys. Status Solidi A **56**, 557 (1979).

[11]K. Schmalz and P. Gaworzewski, Phys. Status Solidi A **64**, 151 (1981).

[12]P. Gaworzewski and K. Schmalz, Phys. Status Solidi A **55**, 699 (1979).

[13]C. S. Fuller and F. H. Doleiden, J. Appl. Phys. **29**, 1264 (1958).

[14]J. W. Cleland, J. Electrochem. Soc. **129**, 2127 (1982).

[15]P. Capper, A. W. Jones, E. J. Wallhouse, and J. G. Wilkes, J. Appl. Phys. **48**, 1646 (1977).

[16]V. Cazcarra and P. Zuino, J. Appl. Phys. **51**, 4206 (1980).

[17]J. Leroueille, Phys. Status Solidi A **67**, 177 (1981).

[18]See, for example, S. M. Sze, *Physics of Semiconductor Devices,* 2nd ed. (Wiley, New York, 1981), p. 27.

[19]C. D. Thurmond, J. Electrochem. Soc. **122**, 1133 (1975).

[20]M. Stavola, J. R. Patel, L. C. Kimerling, and P. E. Freeland, Appl. Phys. Lett. **42**, 73 (1983).

[21]V. N. Mordkovich, Fiz. Tverd. Tela (Leningrad) **6**, 847 (1964) [Sov. Phys—Solid State **6**, 654 (1964)].

[22]V. N. Mordkovich, Fiz. Tverd. Tela (Leningrad) **6**, 2176 (1964) [Sov. Phys.—Solid State **6**, 1716 (1965)].

[23]K. Wada and N. Inoue (unpublished).

[24]L. C. Kimerling and J. L. Benton, Appl. Phys. Lett. **39**, 410 (1981).

[25]The thermal-donor concentration measured by DLTS is reportedly about 1 order of magnitude lower than the added electron concentration. In the present paper, this tendency is also observed. However, concentration itself is not an issue in the present paper.

[26]B. Pajot, H. Compain, J. Lerouille, and B. Clerjaud, Physica **117&118B**, 110 (1983).

[27]K. Graff and H. Pieper, J. Electron. Mater. **4**, 281 (1975).

[28]R. Oeder and P. Wagner, in *Defects in Semiconductors II,* Ref. 4, p. 171.

[29]R. A. Faulkner, Phys. Rev. **184**, 713 (1969).

[30]V. N. Erofeev, V. I. Nikitenko, and V. B. Osvenskii, Phys. Status Solidi **35**, 79 (1969).

[31]J. R. Patel, L. R. Testardi, and P. E. Freeland, Phys. Rev. B **13**, 3548 (1976).

[32]A. J. R. deKock and W. M. van de WiJgert, J. Cryst. Growth **49**, 718 (1980).

[33]A. J. R. deKock and W. M. van de WiJgert, Appl. Phys. Lett. **38**, 888 (1981).

[34]C. W. Pearce and G. Rozgonyi, in *Proceedings of the 1st International Symposium on VLSI Science and Technology* (The Electrochemical Society, Pennington, N. J., 1982), p. 53.

[35]H. Tsuya, Y. Kondo, and M. Kanamori, Jpn. J. Appl. Phys. **22**, L16 (1983).

[36]K. Wada, N. Inoue, and J. Osaka, in *Defects in Semiconductors II,* Ref. 4, p. 126.

[37]F. A. Kroeger, in *Chemistry of Imperfect Crystals,* 2nd ed. (North-Holland, Amsterdam, 1974), Vol. 2, p. 172.